

UDK 546.824, 543.42

## Sol-gel Synthesis of Anatase Nanopowders for Efficient Photocatalytic Degradation of Herbicide Clomazone in Aqueous Media

Aleksandar Golubović<sup>1\*</sup>, Bojana Simović<sup>2</sup>, Slavica Gašić<sup>3</sup>, Dušan Mijin<sup>4</sup>, Aleksandar Matković<sup>1</sup>, Biljana Babić<sup>5</sup>, Maja Šćepanović<sup>1</sup>

<sup>1</sup>Centre for Solid State Physics and New Materials, Institute of Physics, University of Belgrade, Pregrevica 118, 11080 Belgrade-Zemun, Serbia

<sup>2</sup>Institute for Multidisciplinary Research, University of Belgrade, Kneza Višeslava 1, 11000 Belgrade, Serbia

<sup>3</sup>Institute of Pesticides and Environmental Protection, Banatska 31-b, 11080 Belgrade-Zemun, Serbia

<sup>4</sup>Faculty of Technology and Metallurgy, University of Belgrade, Karnegijeva 4, 11000 Belgrade, Serbia

<sup>5</sup>Institute of Nuclear Sciences "Vinča", University of Belgrade, 11001 Belgrade, Serbia

---

### Abstract:

*TiO<sub>2</sub> nanopowders were produced by sol-gel technique using TiCl<sub>4</sub> as a starting material. For the preparation of crystalline anatase with developed surface area, this aqueous solution has been mixed with 0.05 M or 0.07 M (NH<sub>4</sub>)<sub>2</sub>SO<sub>4</sub> solution in a temperature-controlled bath. The pH values of the suspension were 7, 8 or 9. According to the x-ray diffraction (XRD) analysis the anatase crystallite sizes were about 12 nm, which coincided with the average particle size revealed by scanning electron microscopy (SEM).*

*The Raman scattering measurements have shown the presence of a small amount of highly disordered brookite phase in addition to dominant anatase phase with similar nanostructure in all synthesized powders. BET measurements revealed that all synthesized catalysts were fully mesoporous, except the sample synthesized with 0.07 M (NH<sub>4</sub>)<sub>2</sub>SO<sub>4</sub> at pH=9, which had small amount of micropores. The photocatalytic degradation of herbicide Clomazone was carried out for both the pure active substance and ~~as~~ the commercial product (GAMIT 4-EC) under UV irradiation. The best photocatalytic efficiency was obtained for the catalyst with the largest specific surface area, confirming this parameter as crucial for enhanced photocatalytic degradation of the pure active substance and commercial product of herbicide Clomazone.*

**Keywords:** Nanopowder; TiO<sub>2</sub>; Raman spectroscopy; Photodegradation; Clomazone.

---

## 1. Introduction

Nanocrystalline titanium dioxide (TiO<sub>2</sub>) is probably the most studied nanomaterials due to stability of its chemical structure, biocompatibility, optical, electronic, porous, and

---

\*<sup>1</sup> Corresponding author: [golubovic@ipb.ac.rs](mailto:golubovic@ipb.ac.rs)

photocatalytic properties [1]. In spite of this, finding the optimum synthesis condition for producing TiO<sub>2</sub> nanoparticles suitable for some specific applications still represents technological challenge and attracts the considerable attention of the scientific community. Because of relatively good control over the synthesis parameters, and their impact on TiO<sub>2</sub> particle phase, shape, size and surface properties, the sol-gel synthesis technique is highly favoured [2, 3]. It is crucial to note that any changes in sol-gel synthesis conditions, however small, could provoke significant effects on the synthesised nanoparticles which deserve to be thoroughly investigated [4]. Besides that, TiO<sub>2</sub> is the very important constituent of composite ceramic materials (binary, as Al<sub>2</sub>O<sub>3</sub>-TiO<sub>2</sub> and TiO<sub>2</sub>-Y<sub>2</sub>O<sub>3</sub> or ternary, as Al<sub>2</sub>O<sub>3</sub>-TiO<sub>2</sub>-Y<sub>2</sub>O<sub>3</sub>) [5], and getting acquainted with properties and abilities for applying can be necessary for possibility of composite applications.

The pesticides have an important role in agriculture, but they can have a negative impact on the environment, particularly because of the possibility of water pollution. This is the reason for a great public concern regarding the water contamination by pesticides in recent times. The Clomazone (2-[(2-chlorophenyl) methyl]-4, 4-dimethyl-3-isoxazolidinone, CAS 81777-89-1) is herbicide which has been applied against different kind of weeds for many years. It is highly water soluble (1.100 g/l), weakly to moderately persistent in soil with half-life ranging from 5 to 60 days, depending on the soil type and environmental conditions, weakly sorptive to soil ( $K_d = 0.47-5.30$  mg/l), with organic carbon partition coefficient  $K_{oc}$  of 150 mg/l [6, 7]. All these properties indicate that Clomazone has the potential for water contamination. Indeed, detection of Clomazone residues in a large number of water samples collected from rivers in rice cultivation regions has been confirmed [8]. On the other side, pesticides are rarely used as pure materials. Namely, active substances are usually mixed with various inert ingredients to produce commercial products, meaning that during the application commercial products come into the environment; instead of pure active substance. However, the rate of degradation of pure active substance and commercial products which are made by them might be different [9]. So, in our study we compare both the photodegradation of the pure active substance and the commercial product (GAMIT 4-EC) of herbicide Clomazone.

There are various processes for contaminated water treatment and the photodegradation in suspension with TiO<sub>2</sub> seems to be the promising one among them. Photocatalytic activity of TiO<sub>2</sub> catalyst can be influenced by many factors (content, crystallinity and stoichiometry of the anatase phase; particle size and microstrain; surface area, pore size distribution and shape; the amount of surface O-H groups and other surface properties [3, 10]), but decisive factor for enhanced photocatalytic efficiency in degradation of different pollutants could not be the same. In our study we used the same duration of the UV irradiation as it has been done in the literature for the Clomazone in the present of TiO<sub>2</sub> catalyst, but our aqueous media was distilled water (not natural water as used before as we want to eliminate the influence of natural water to the process of photodegradation) [11].

Literature shows that TiO<sub>2</sub> synthesized using (NH<sub>4</sub>)<sub>2</sub>SO<sub>4</sub> as auxiliary compound has good catalytic performance when used for photodegradation of herbicide Bentazon [12]. While characteristics of synthesized TiO<sub>2</sub> were not compared with commercial one, it is showed that synthesized anatase phase has better photocatalytic efficiency than rutile phase. Although this fact does not indicate that same will be achieved in the case of Clomazone, we went a step further and test it with an additional variations in the concentration of (NH<sub>4</sub>)<sub>2</sub>SO<sub>4</sub> and pH during the TiO<sub>2</sub> synthesis. The results of XRD analysis and Raman scattering measurements have shown similar structural and compositional properties of produced nanopowders, whereas BET measurements have revealed considerable variation in their specific surface area. This allowed us to systematically investigate the influence of developed specific surface area of synthesized TiO<sub>2</sub> catalysts on photodegradation of both pure active substance and the commercial product with the same active ingredients (Clomazone).

## 2. Experimental

### 2.1. Materials and methods

All reagents were of analytical grade, obtained from commercial sources and used without further purification. Titanium tetrachloride ( $\text{TiCl}_4$ , Merck Chemicals) has been used as the starting material in sol-gel technique, along with ammonium sulphate ( $(\text{NH}_4)_2\text{SO}_4$ , Kemika), and ammonium hydroxide ( $\text{NH}_4\text{OH}$ , Carlo Erba). For the preparation of crystalline anatase, this aqueous suspension was mixed with 0.05 M or 0.07 M  $(\text{NH}_4)_2\text{SO}_4$  solution in a temperature-controlled bath. The pH of the suspensions were 7, 8 or 9. Calcination was carried out at 510 °C during 2 hours. The heating and cooling rates were the same, 135 °C/h. Obtained samples were labelled by the letter L or H (for low and high concentration of  $(\text{NH}_4)_2\text{SO}_4$ , respectively) and the number related to the pH value of suspension.

Technical substance Clomazone was purchased from Shenzhen Yancheng Chemicals Co., China, with decelerated purity of 95 % (min.), whereas Gamit 4-EC (emulsifiable concentrate, active ingredient Clomazone 480 g/L, producer: FMC Corporation, USA) were used as commercial product.

### 2.2. Characterization techniques

Room temperature X-ray powder diffraction (XRD) patterns were collected on an ITAL Structures APD2000 X-ray diffractometer using Cu  $K\alpha$  radiation ( $\lambda = 1.5418 \text{ \AA}$ ) in  $2\theta$  range of 20–80°.

The SEM measurements were carried out on a Tescan MIRA3 field emission gun SEM, at 25 kV in high vacuum. Before the measurements the powder was sonicated in ethanol for 5 minutes. Immediately afterwards, a drop of solution was casted onto a freshly cleaved kish graphite crystal embedded with a silver paste into a SEM sample holder. Excess material was removed in a stream of argon gas and the sample was left to degas in low vacuum for 30 minutes.

The Raman scattering measurements were performed on the synthesized powders pressed into pellets, by using TriVista 557 triple spectrometer with the 900/900/1800 grooves/mm gratings in backscattering micro-Raman configuration. All Raman spectra were recorded at room temperature in the air using 514.5 nm line of a mixed  $\text{Ar}^+/\text{Kr}^+$  gas laser.

Adsorption and desorption isotherms of  $\text{N}_2$  were measured on powders, at 196 °C, using the gravimetric McBain method. The specific surface area,  $S_{\text{BET}}$ , pore size distribution, mesopore including external surface area,  $S_{\text{meso}}$ , and micropore volume,  $V_{\text{mic}}$ , were calculated from the isotherms of the powders. Pore size distribution was estimated by applying Barrett-Joyner-Halenda (BJH) method [13] to desorption branch of the isotherms, whereas mesopore surface and micropore volume were estimated using the high resolution  $\alpha_s$  plot method [14-16]. Micropore surface,  $S_{\text{mic}}$ , was calculated by subtracting  $S_{\text{meso}}$  from  $S_{\text{BET}}$ .

The photocatalytic degradation of the pure active substance and commercial product (GAMIT 4-EC) of herbicide Clomazone (0.05 mM) in aqueous suspensions of the synthesized and the commercial (Degussa P25)  $\text{TiO}_2$  were examined under UV irradiation (Osram Ultra Vitalux® 300 W lamp - ratio of UV-A and UV-B lights of 13.6:3). In a typical experiment, 25 mL of a solution (0.05 mM) was used, the quantity of  $\text{TiO}_2$  was 12.5 mg, and agitation for 60 min was applied in a dark by continuous stirring at 400 rpm to keep the suspension homogenous. Then, the lamp was switched on and the suspension sampled after appropriate time of irradiation (every 10 min). The concentration of pollutants was determined after centrifugation of the sample at 6000 rpm by UV-Vis spectrophotometer (Shimadzu 1700) at appropriate wavelength.

### 3. Results and discussion

#### 3.1. Synthesis

The TiO<sub>2</sub> anatase phase was prepared by sol-gel technique using TiCl<sub>4</sub> as a starting material according to the procedure described in our previous paper [10, 17]. For producing the nanopowders with developed specific surface area, solution of (NH<sub>4</sub>)<sub>2</sub>SO<sub>4</sub> was used [12].

#### 3.2. Structure, morphology and phase composition of synthesized nanopowders

The XRD patterns of all prepared samples (Fig. 1) are readily indexed to the anatase TiO<sub>2</sub> phase (anatase tetragonal type structure, PDF card 84-1285,  $a = 3.7848 \text{ \AA}$ ,  $c = 9.5124 \text{ \AA}$ ,  $V = 136.26 \text{ \AA}^3$ , space group I41/amd (141)). As can be seen from Fig. 1, diffractograms of all samples are very similar. The unit cell parameters obtained from the XRD analysis by Jade computer program, together with the values of average crystallite size and microstrain calculated by Scherrer and Williamson-Hall methods are presented in Table I. It can be seen that variation of the anatase unit cell parameters did not exceed  $0.02 \text{ \AA}$ , whereas average anatase crystallite size is in the range of  $11.5 \pm 1 \text{ nm}$  for all synthesized samples. In addition to the anatase diffraction peaks, a low-intensity diffraction peak at  $2\theta \approx 30.9^\circ$ , which can be ascribed to the brookite phase of TiO<sub>2</sub> [17], is observed in the XRD patterns of the powders synthesized with pH=7.

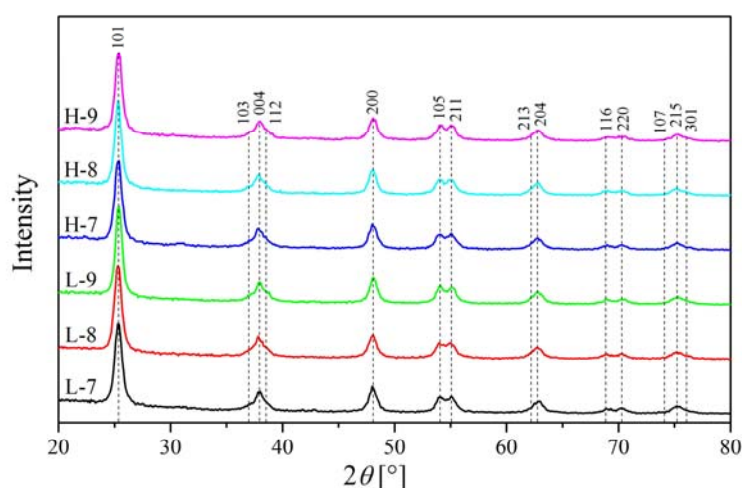


**Fig. 1.** XRD patterns of all prepared samples.

**Tab. I** The unit cell parameters, the average crystallite size  $\langle D \rangle$  and microstrain of anatase phase in synthesized TiO<sub>2</sub> nanopowders estimated by Scherrer and Williamson-Hall methods.

Sample name	Unit cell parameters		Scherrer method	Williamson-Hall method	
	a [ $\text{\AA}$ ]	c [ $\text{\AA}$ ]	$\langle D \rangle$ [nm]	$\langle D \rangle$ [nm]	Microstrain [%]
L-7	3.7915(2)	9.4972(5)	10.6(2)	10.9(7)	0.03(7)
L-8	3.7872(2)	9.5081(5)	10.4(2)	10.9(8)	0.07(9)
L-9	3.7798(1)	9.4966(5)	12.0(2)	12.5(7)	0.04(6)
H-7	3.7904(1)	9.4993(5)	10.4(2)	10.8(9)	0.10(1)
H-8	3.7873(2)	9.4890(4)	11.8(2)	12.3(8)	0.05(6)
H-9	3.7765(1)	9.4902(5)	11.2(2)	11.9(8)	0.06(7)

The SEM image and particle size histogram of the sample H-9, as the representative ones, are shown in Fig. 2a and Fig. 2b, respectively. These results have revealed that most of the particles in this sample were of spherical shape. The average value of particle diameter was about 12 nm. Coincidence between average value of particles diameter estimated by SEM and anatase crystallite size evaluated from XRD analysis by Williamson-Hall method has pointed out that obtained particles are monocrystalline.

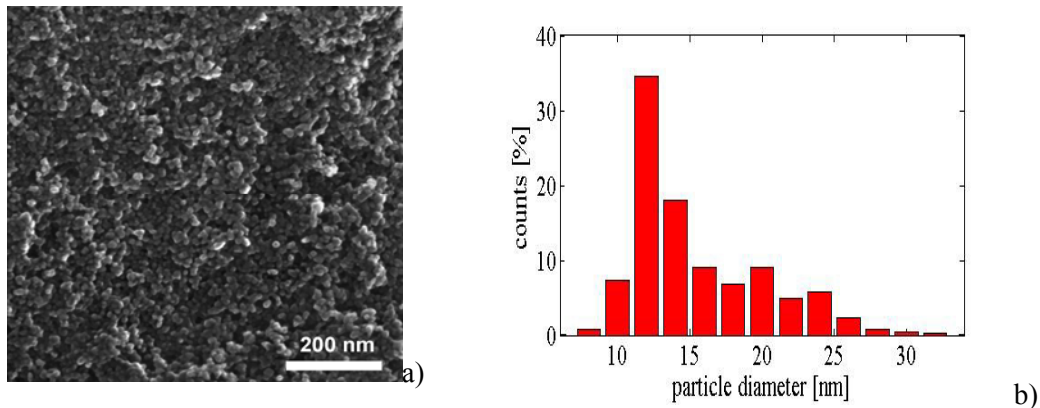


**Fig. 2.** a) SEM image of TiO<sub>2</sub> (sample H-9) with 800-x magnification. Scale bar is 200 nm; b) Particle size histogram of the sample H-9 obtained from SEM data.

Nitrogen adsorption isotherms for all samples, as the amount of N<sub>2</sub> adsorbed in a function of relative pressure at -196 °C, are shown in Fig. 3. According to the IUPAC classification [18] isotherms of samples are of type IV and with a hysteresis loop which is associated with mesoporous materials. The observed type H2 shape of hysteresis loop indicates a poorly defined shape of pores [19]. As listed in Table II, the specific surface area calculated by BET equation,  $S_{\text{BET}}$ , lies within the range of 54-85 m<sup>2</sup> g<sup>-1</sup> for all samples, with the exception of the sample H-9 where reaches the value of 181 m<sup>2</sup> g<sup>-1</sup>.

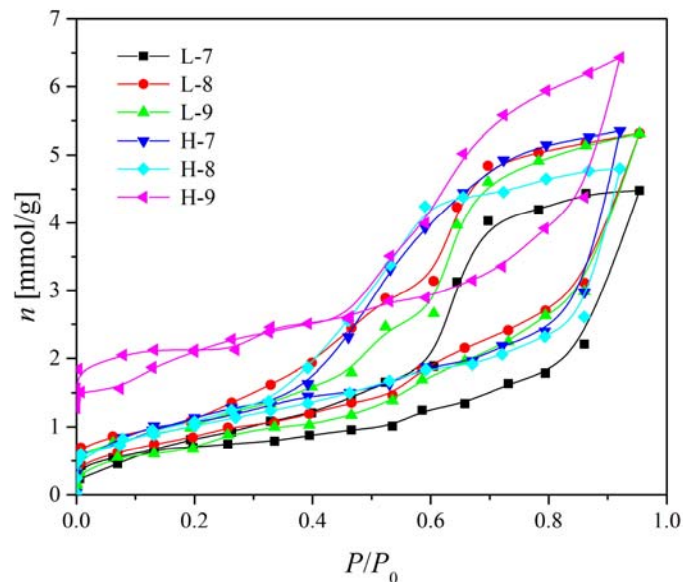


**Fig. 3.** Nitrogen adsorption isotherms, as the amount of N<sub>2</sub> adsorbed as function of relative pressure for TiO<sub>2</sub> nanopowders. Solid symbols - adsorption, open symbols – desorption.

Pore size distribution (PSD) estimated by BJH method is shown in Fig. 4. The figure shows that all samples are mesoporous, with bimodal PSD for samples L 7-9 and H-9. The most of the pores radii lies between 1.5 and 6.0 nm.

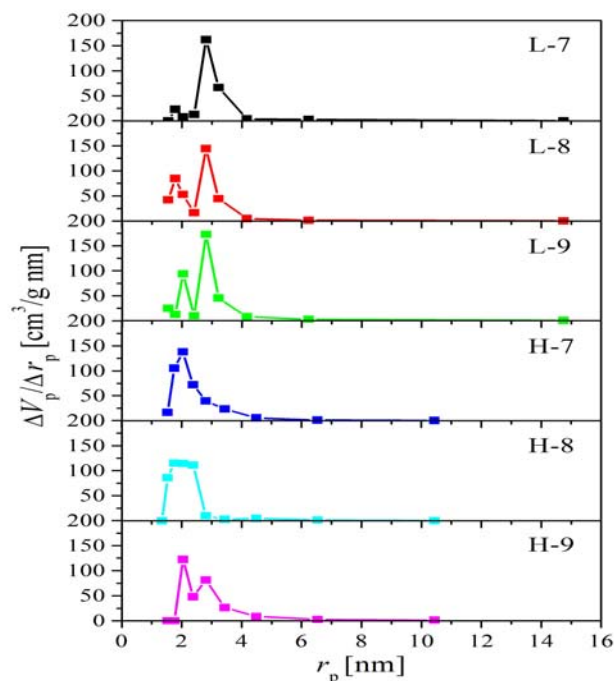


**Fig. 4.** Pore size distribution (PSD) synthesized  $\text{TiO}_2$  nanopowders.

The  $\alpha_s$  plots, obtained on the basis of the standard nitrogen adsorption isotherm are shown in Fig. 5. The slope of straight line in the high  $\alpha_s$  region gives a mesoporous surface area, including the contribution of external surface,  $S_{\text{meso}}$ , whereas micropore volume,  $V_{\text{mic}}$ , is given by the  $y$ -intercept of this line. Calculated values of porosity parameters ( $S_{\text{meso}}$ ,  $S_{\text{mic}}$ ,  $V_{\text{mic}}$ ), given in Table II confirm that samples L 7-9 and H 7-8 are mesoporous, whereas the sample H-9 (with the highest  $S_{\text{BET}}$ ) has a certain amount of micropores.

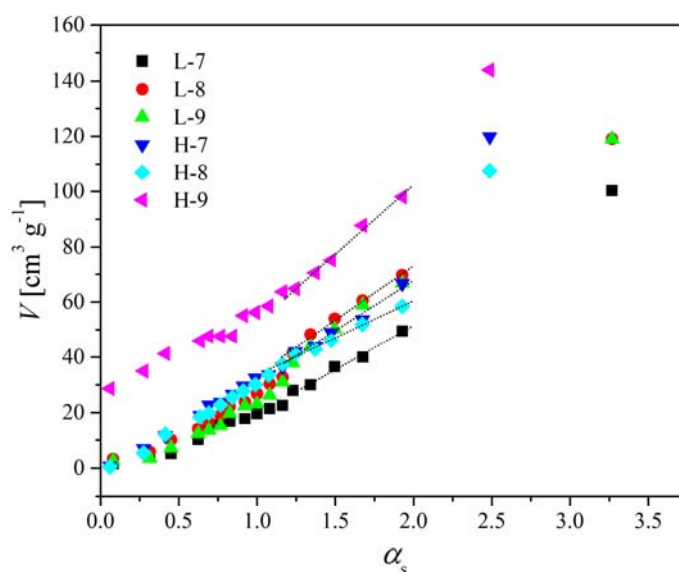


**Fig. 5.**  $\alpha_s$  – Plot for nitrogen adsorption isotherm of synthesized  $\text{TiO}_2$  nanopowders.

**Tab. II** The pore size distribution for synthesized TiO<sub>2</sub> nanopowders.

Sample	$S_{\text{BET}}$ [m <sup>2</sup> /g]	$S_{\text{meso}}$ [m <sup>2</sup> /g]	$S_{\text{mic}}$ [m <sup>2</sup> /g]	$V_{\text{mic}}$ [cm <sup>3</sup> /g]
L-7	56	56	-	-
L-8	66	66	-	-
L-9	54	54	-	-
H-7	85	85	-	-
H-8	81	81	-	-
H-9	181	126	55	0.014

The Raman spectra of synthesized TiO<sub>2</sub> powders are shown in Fig. 6. In all spectra dominant Raman modes can be assigned to the Raman active modes of the anatase crystalline phase [20]:  $\sim 146$  cm<sup>-1</sup> ( $E_g$ ),  $199$  cm<sup>-1</sup> ( $E_g$ ),  $399$  cm<sup>-1</sup> ( $B_{1g}$ ),  $519$  cm<sup>-1</sup> (combination of  $A_{1g}$  and  $B_{1g}$  that cannot be resolved at room temperature) and  $639$  cm<sup>-1</sup> ( $E_g$ ). Similar position ( $\sim 146$  cm<sup>-1</sup>) and linewidth ( $\sim 12$  cm<sup>-1</sup>) of the most intensive  $E_g$  anatase Raman mode for all investigated TiO<sub>2</sub> samples indicate that anatase crystallites in all powders have similar nanosizes and structure [10, 17]. As can be seen from the inset of Fig. 6, low intensity modes of TiO<sub>2</sub> brookite phase is also observed in the spectra of all synthesized samples:  $A_{1g}$  ( $\sim 247$  cm<sup>-1</sup>),  $B_{3g}$  ( $\sim 288$  cm<sup>-1</sup>),  $B_{1g}$  ( $\sim 322$  cm<sup>-1</sup>), and  $B_{2g}$  ( $\sim 366$  cm<sup>-1</sup>) [10, 21]. Low intensities and large widths of these modes indicate great disorder and partial amorphization of brookite in all samples. The ratio of the sum of the integrated intensities of Lorentzian peaks associated with the brookite modes ( $\Sigma I_B$ ), to the integrated intensity of Lorentzian peak related to the  $B_{1g}$  mode of anatase phase ( $I_{A(B_{1g})}$ ), could be used as a rough indicator of brookite content in the TiO<sub>2</sub> samples [10]. The variation of the  $\Sigma I_B/I_{A(B_{1g})}$  intensity ratio with pH and concentration of (NH<sub>4</sub>)<sub>2</sub>SO<sub>4</sub> in aqueous suspension during the synthesis of nanopowders is shown in Fig. 7. These results have confirmed a tendency of reducing of brookite content with increase of pH value during the synthesis, observed in our earlier investigations [17]. Also, it appears that higher concentration of (NH<sub>4</sub>)<sub>2</sub>SO<sub>4</sub> in aqueous suspension causes an increase of the brookite phase content in samples, although it should be noted that  $\Sigma I_B/I_{A(B_{1g})}$  ratio could depend not only on the brookite/anatase phase composition but also on the crystallinities of both TiO<sub>2</sub> phases.

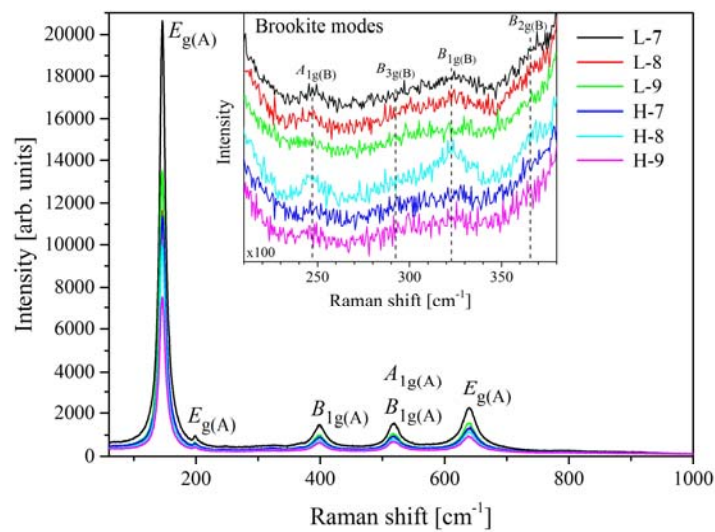
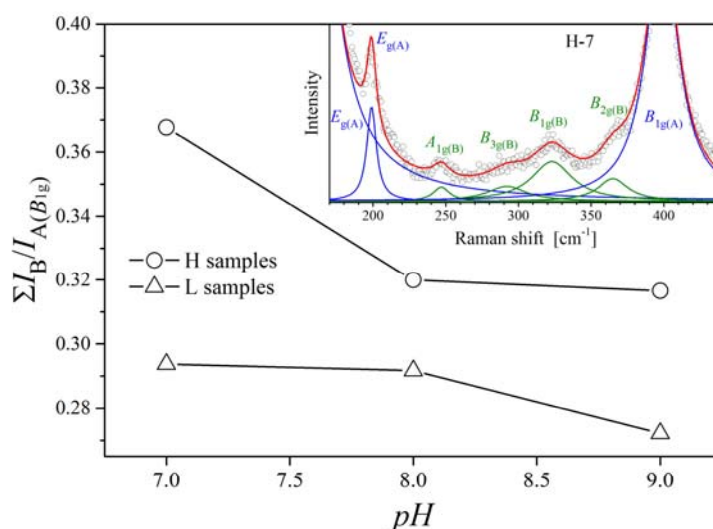


Fig. 6. Raman spectra of synthesized TiO<sub>2</sub> powders with denoted characteristic anatase modes (A). The inset: Brookite Raman modes (B) in the same spectra normalized on the intensity of  $B_{1g}(A)$  anatase mode, enlarged and upshifted for clarity.



**Fig. 7.** Dependence of the ratio between the total brookite Raman modes intensity,  $\Sigma I_B$ , and the anatase  $B_{1g}$  mode intensity,  $I_{A(B1g)}$ , on pH during the synthesis of  $\text{TiO}_2$  nanopowders in the presence of  $(\text{NH}_4)_2\text{SO}_4$  aqueous solution with concentration of 0.05 M (L) and 0.07 M (H). The inset: Lorentzian fit of some anatase and brookite modes in the  $170\text{--}440\text{ cm}^{-1}$  range of experimental Raman spectra of the sample H-7.

### 3.3. Photocatalytic degradation

The photocatalytic degradation of pure active substance and commercial product (GAMIT 4-EC) of herbicide Clomazone (0.05 mM) in aqueous suspensions has been studied using the synthesized  $\text{TiO}_2$  nanopowders under UV irradiation. The results were compared to photodegradation accomplished under the same conditions by using commercial nanopowder (Degussa P25), which was proved to be efficient catalyst in photodegradation of various pollutants, including Clomazone [11, 22]. Our experiments have shown that 69 % of initial Clomazone amount was degraded after 60 min of photodegradation reaction, whereas only 55 % of initial substance was removed when the commercial product GAMIT 4-EC was treated (Figs. 8 and 9).

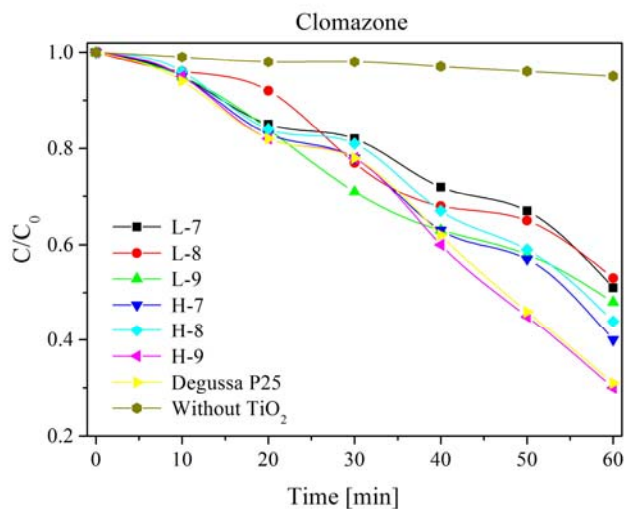


**Fig. 8.** The kinetics of degradation of Clomazone under UV irradiation monitored in the presence of synthesized  $\text{TiO}_2$  nanopowders and Degussa P25.

Among sol-gel synthesized TiO<sub>2</sub> catalysts, the H-9 nanopowder, prepared using suspension of pH=9 and (NH<sub>4</sub>)<sub>2</sub>SO<sub>4</sub> concentration of 0.07 M, has shown the highest photocatalytic efficiency in degradation of both pure active substance and the commercial product of Clomazone. This catalyst removed 70 % of the pure active substance (Fig. 8) and 57% of GAMIT 4-EC (Fig. 9) after 60 minutes of photocatalytic reaction under UV irradiation, which made H-9 a little more efficient than Degussa P25 in degradation of both substances.

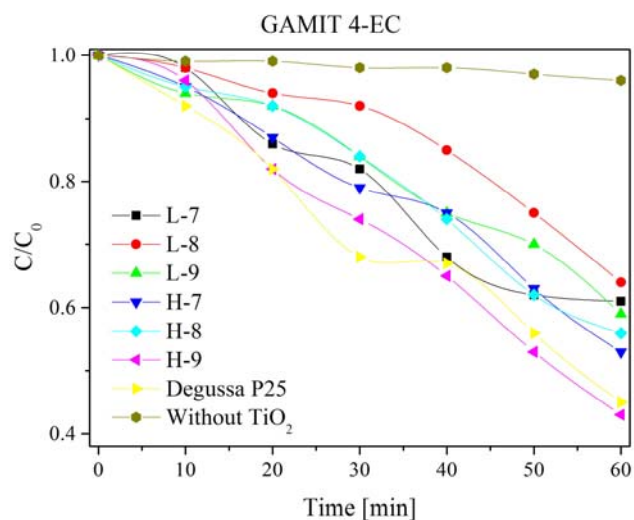


**Fig. 9.** The kinetics of degradation of GAMIT 4-EC under UV irradiation monitored in the presence of synthesized TiO<sub>2</sub> nanopowders and Degussa P25.

Different photocatalytic efficiency in degradation of pure active substance of Clomazone and the commercial product GAMIT 4-EC may be explained by the fact that GAMIT 4-EC (contain) possesses, beside Clomazone, other inert ingredients (such as emulsifiers, solvent and so on) that could affect the rate of photocatalytic degradation by reaction with hydroxyl radicals, or by adsorbing to the catalyst surface.

The main factor accountable for the enhanced efficiency of the H-9 catalyst in photodegradation of Clomazone could be found in its developed specific surface area. Namely, the BET measurements revealed  $S_{\text{BET}}$  of 181 m<sup>2</sup>/g for this nanopowder, which is more than two times larger than  $S_{\text{BET}}$  for the other synthesized nanopowders. This finding is consistent with the results of the test with hole and •OH radical scavengers which indicated that in the photodegradation of Clomazone the surface degradation mechanism has played a crucial role [22].

#### 4. Conclusions

TiO<sub>2</sub> nanopowders were prepared by sol-technique using TiCl<sub>4</sub> as a starting material and (NH<sub>4</sub>)<sub>2</sub>SO<sub>4</sub> for obtaining nanopowders with developed specific surface area. In experiments of synthesis three various pH of suspension were applied (7, 8 and 9) and two concentrations of (NH<sub>4</sub>)<sub>2</sub>SO<sub>4</sub> (0.05M and 0.07 M). XRD analysis has shown that all synthesized powders were dominantly in anatase phase with average crystallite size of about 12 nm, which coincided with average particle size revealed by SEM. The Raman scattering measurements have shown the presence of a small amount of highly disordered brookite phase in addition to the dominant anatase phase with similar nanostructure in all synthesized powders. The photocatalytic degradation of the pure active substance and commercial product (GAMIT 4-EC) of herbicide Clomazone (0.05 mM) in aqueous suspensions of synthesized or commercial (Degussa P25) TiO<sub>2</sub> nanopowders were examined under UV irradiation. The

highest photocatalytic efficiency was obtained for the nanopowder synthesized using suspension of pH=9 and 0.07 M (NH<sub>4</sub>)<sub>2</sub>SO<sub>4</sub>. This nanopowder had the largest  $S_{\text{BET}}$  among all synthesized nanopowders, which has pointed to specific surface area as the main factor accountable for the enhanced efficiency of the sol-gel synthesized TiO<sub>2</sub> nanopowders in photocatalytic degradation of pure active substance of Clomazone and its commercial product GAMIT 4-EC.

## Acknowledgements

Support of this work by the Ministry of Education, Science and Development of the Republic of Serbia under the Grant No. III45018 is gratefully acknowledged.

## 5. References

1. D. P. Macwan, P. N. Dave, S. Chaturvedi, "A review on nano-TiO<sub>2</sub> sol-gel type syntheses and its applications", *J. Mater. Sci.*, 46 (2011) 3669–3686.
2. S. Sakka, (ed.), *Handbook of sol-gel science and technology*, Vol. 1: Sol-gel processing, (2005) Dordrecht: Kluwer.
3. H. Jensen, A. Solovieva, Z. Lib, E. G. Søgaard, "XPS and FTIR investigation of the surface properties of different prepared titania nano-powders", *Appl. Surface Sci.*, 246 (2005) 239–249.
4. J. Lind, "Effect of synthesis duration and HCl acid concentration on the formation of hydrothermally synthesised TiO<sub>2</sub> nanoparticles", Master Thesis, Faculty of Engineering, Cape Peninsula University of Technology, Cape Town Campus, July 2015.
5. M. Vlasova, M. Kakazey, P. A. Márquez Aguilar, E. A. Juarez-Arellano, R. Guardian Tapia, V. Stetsenko, A. Bykov, S. Lakiza, A. Ragulya, *Sci. Sinter.*, 45 (2013) 247-259.
6. R. Zanella, E. G. Primel, F.F. Gonçalves, A. F. Martins, "Development and validation of a high-performance liquid chromatographic method for the determination of Clomazone residues in surface water", *J. Chromatogr. A*, 904 (2000) 257-262.
7. J. P. Cumming, R. B. Doyle, P.H. Brown, "Clomazone dissipation in four Tasmanian topsoils", *Weed Sci.*, 50 (2002) 405-409.
8. E. Marchesan, R. Zanella, L. A. de Avila, E. Rabaioli Camargo, S. L. de Oliveira Machado, V. R. Mussoi Macedo, "Rice herbicide monitoring in two Brazilian rivers during the rice growing season", *Sci. Agr.*, 64 (2007) 131-137.
9. P. L. Huston, J. J. Pignatello, "Degradation of selected pesticide active ingredients and commercial formulations in water by photo-assisted fenton reaction", *Wat. Res.*, 33 (1999) 1238-1246.
10. M. Šćepanović, B. Abramović, A. Golubović, S. Kler, M. Grujić-Brojčin, Z. Dohčević-Mitrović, B. Babić, B. Matović, Z. V. Popović, "Photocatalytic degradation of metoprolol in water suspension of TiO<sub>2</sub> nanopowders prepared using sol-gel route", *J. Sol-Gel Sci. Technol.*, 61 (2012) 390–402.
11. B. F. Abramović, V. N. Despotović, D. V. Šojic, D. Z. Orčić, J. J. Csanádi, D. D. Četojevic-Simin, "Photocatalytic degradation of the herbicide Clomazone in natural water using TiO<sub>2</sub>: Kinetics, mechanism, and toxicity of degradation products", *Chemosphere*, 93 (2013) 166–171.

12. R. Pourata, A. R. Khataee, S. Aber, N. Daneshvar, "Removal of the herbicide Bentazon from contaminated water in the presence of synthesized nanocrystalline TiO<sub>2</sub> powder under irradiation of UV-C light", *Desalination*, 249 (2009) 301-307.
13. E. P. Barrett, L. G. Joyner, P. P. Halenda, "[The determination of pore volume and area distributions in porous substances. I. Computations from nitrogen isotherms](#)", *J. Am. Chem. Soc.*, 73 (1951) 373-380.
14. K. Kaneko, C. Ishii, M. Ruike, H. Kuwabara, "Origin of superhigh surface area and microcrystalline graphitic structures of activated carbons", *Carbon*, 30 (1992) 1075-1088.
15. M. Kruk, M. Jaroniec, K. P. Gadakaree, "Nitrogen adsorption studies of novel synthetic active carbons", *J. Colloid. Interface. Sci.*, 192 (1997) 250-256.
16. K. Kaneko, C. Ishii, H. Kanoh, Y. Hanzawa, N. Setoyama, T. Suzuki, "Characterization of porous carbons with high resolution  $\alpha_s$ -analysis and low temperature magnetic susceptibility", *Adv. Colloid Interface Sci.*, 76-77 (1998) 295-320.
17. A. Golubović, M. Šćepanović, A. Kremenović, S. Aškračić, V. Berec, Z. Dohčević-Mitrović, Z. V. Popović, "Raman study of the variation in anatase structure of TiO<sub>2</sub> nanopowders due to the changes of sol-gel synthesis conditions", *J. Sol-Gel Sci. Technol.*, 49 (2009) 311-319.
18. K. S. W. Sing, D. H. Everett, R. A. W. Haul, L. Moscou, R. A. Pierotti, J. Rouquerol, T. [Siemieniowska](#), "Reporting physisorption data for gas/solid systems with special reference to the determination of surface area and porosity", *Pure Appl. Chem.* 57 (1985) 603-619.
19. S. Lowell, J. E. Shields, M. A. Thomas, M. Thommes, "Characterization of Porous Solids and Powders: Surface Area, Pore Size and Density", Ed. Kluwer Academic Publishers, Dordrecht Netherlands, 2004, p. 44.
20. T. Ohsaka, F. Izumi, Y. Fujiki, "Raman spectrum of anatase, TiO<sub>2</sub>", *J. Raman spectrosc.*, 7 (1978) 321-324.
21. G. A. Tompsett, G. A. Bowmaker, R. P. Cooney, J. B. Metson, K. A. Rodgers, J. M. Seakins, "The Raman spectrum of brookite, TiO<sub>2</sub> (*Pbca*, *Z* = 8)", *J. Raman Spectrosc.*, 26 (1995) 57-62.
22. B. Abramović, V. Despotović, D. Šojic, N. Finčur, "Mechanism of clomazone photocatalytic degradation: hydroxyl radical, electron and hole scavengers", *Reac. Kinet. Mech. Cat.*, 115 (2015) 67-79.

---

**Садржај:** TiO<sub>2</sub> нанопрахови су добијени сол-гел техником коришћењем TiCl<sub>4</sub>. При припреми кристалита анатаса са развијеном специфичном површином, TiCl<sub>4</sub> раствор је са 0.05 M или 0.07 M раствором (NH<sub>4</sub>)<sub>2</sub>SO<sub>4</sub> у температурно контролисаном купатилу при pH 7, 8 или 9. Дифрактометријска анализа је показала величину кристалита анатаса од око 12 nm, што је у сагласности са средњом величином честица утврђених на основу SEM-а. Мерења Раманском спектроскопијом су показала присуство мале количине брукитне фазе ниске уреджености и доминантну анатас фазу са сличном наноструктуром у свим синтетисаним праховима. BET мерења су показала да су сви синтетисани катализатори мезопорозне структуре, осим узорка синтетисаног са 0.07 M (NH<sub>4</sub>)<sub>2</sub>SO<sub>4</sub> при pH=9, у којем је нађена мала количина микропора. Фотокаталитичка деградација хербицида Клоламос (чиста активна супстанца и комерцијални производ GAMIT 4-EC) је извршена под UV озрачивањем. Највећа фотокаталитичка ефикасност, већа од комерцијалног производа Degussa P25, је добијена за катализатор са највећом специфичном површином, потврђујући да је

---

*тај параметар кључни фактор фотокаталитичке деградације чисте активне супстанце и комерцијалног производа хербицида Кломазон.*

***Кључне речи:*** *нанопрах; TiO<sub>2</sub>; Раманска спектроскопија; фотодеградиција; Кломазон.*

---

© 2016 Authors. Published by the International Institute for the Science of Sintering. This article is an open access article distributed under the terms and conditions of the Creative Commons — Attribution 4.0 International license (<https://creativecommons.org/licenses/by/4.0/>).

